CHEMICAL ENGINEERING TRANSACTIONS
VOL. 96, 2022
A publication of AIDIC
The Italian Association of Chemical Engineering
Online at www.cetjournal.it
Guest Editors: David Bogle, Flavio Manenti, Piero Salatino

ISBN 978-88-95608-95-2; **ISSN** 2283-9216
DOI: 10.3303/CET2296054

Dynamic Multi-Objective Optimization Applied to Biomethanation Process

Juan C. Acosta-Pavas[a], Carlos E. Robles-Rodríguez[a], Camilo A. Suarez Méndez[b], Jérôme Morchain[a]*, Claire Dumas[a], Arnaud Cockx[a], César A. Aceves-Lara[a,]*

[a]TBI, Université de Toulouse, CNRS, INRAE, INSA, Toulouse, France
[b]Universidad Nacional de Colombia, Medellín, Carrer 65 No. 59a-110, 050034 Medellín, Colombia
aceves@insa-toulouse.fr

Dynamic mathematical models could be beneficial for understanding and simulating processes to achieve an optimal operation. The optimum, however, could depend on several variables that can be conflicting. In this regard, Dynamic Multi-objective Optimization (DMO) is necessary for the trade-off between several objectives. This work aims at proposing a DMO as a control strategy integrating two optimization problems. The objective is to maximize the yield and productivity of the biomethanation processes by modifying the inlet liquid and injected gas flowrates. First, multi-objective optimization was applied. Three Pareto optimal points were selected to develop five cases in dynamic optimization. Case 1 corresponded to experimental data. Cases 2, 3, and 4 considered as objectives the maximum productivity, maximum productivity and yield, and maximum yield, respectively. Case 5 was performed to assess a switch between objectives. For case 3, the yield decreased to 0.97 times, while the productivity increased 3.26 times with respect to case 1. The injected gas flowrate ranged from 2.69 to 8.43 m^3/d, and the inlet liquid flowrate reached an approximate value of 7.0×10^{-3} m^3/d. These results showed the feasibility and good efficiency of the proposed methodology.

1. Introduction

The use of dynamic models allows to gain a better understanding of different biological processes. One of those processes is biomethanation, in which organic matter, such as agricultural residues, organic effluents from the food industry, animal manure, or waste/wastewater residues are transformed through the synergistic work of a variety of microorganisms into a mixture of CH_4, and CO_2 (Dar *et al.*, 2021). This process was first modeled by using the well-known Anaerobic Digestion Model No. 1 (ADM1) (Batstone *et al.*, 2002). This model has been adapted to solve stiffness problems (Rosen and Jeppsson, 2006), variation of pH (Czatzkowska *et al.*, 2020), and the inclusion of gas injection to obtain high purity methane (Sun *et al.*, 2021). However, managing the biomethanation process is still an arduous task due to the multiple molecules and different microorganisms involved. As a result, obtaining desired objectives, such as high yields, high productivities, low processing times or low flowrates remains difficult at an industrial scale, especially when you need to optimize several of them simultaneously. The use of dynamic models plays a crucial role in the design of control strategies, e.g., optimal control, adaptive control, or model predictive control (MPC) (Morales-Rodelo *et al.*, 2020) to maintain the value of the variables of interest during the process or to optimize several variables, i.e., a multi-objective optimization (MO). When we talk about MPC, we refer to optimal controllers, i.e., the control action responds to the optimization of a criterion (cost function), which is related to the future behavior of the system, determined from the dynamic model (Camacho and Bordons, 2007). MO involves multiple criteria decision making, i.e., it implies optimizing problems where there are more than one variable to be optimized simultaneously, and those variables are usually conflictive (Chang, 2015; Vertovec *et al.*, 2021). In this context, an optimal solution set that fulfills the desired conditions of the conflicting variables is established and selected as Pareto optimal set. If a solution point is not dominated by another solution, it is considered a Pareto Optimal Point (POP). Therefore, it is ideal to have the highest number of Pareto optimal solutions (Deb *et al.*, 2002).

Paper Received: 18 January 2022; Revised: 18 August 2022; Accepted: 14 July 2022
Please cite this article as: Acosta-Pavas J.C., Robles-Rodríguez C.E., Suarez Méndez C.A., Morchain J., Dumas C., Cockx A., Aceves-Lara C.A., 2022, Dynamic Multi-objective Optimization Applied to Biomethanation Process, Chemical Engineering Transactions, 96, 319-324 DOI:10.3303/CET2296054

This work aims at proposing a Dynamic Multi-objective Optimization (DMO) to find the trade-off between the maxima of yield and productivity of the biomethanation process through a Pareto optimal set. Afterwards, a POP is selected and used as the optimal reference trajectory. Then, a dynamic optimization is formulated in terms of a MPC to modify the inlet liquid and injected gas flowrates to achieve the optimal values of yield and productivity obtained from the POP.

2. Biomethanation Model Extension Proposal

The biomethanation process can be divided in four phases: hydrolysis, acidogenesis, acetogenesis and methanogenesis (Dar *et al.*, 2021). In the first phase, the fermentative bacteria excrete enzymes that hydrolyse complex organic polymers (carbohydrates, proteins, and lipids) into soluble monomers, such as monosaccharides, amino acids, and long chain fatty acids. In the second phase, these monomers are transformed into volatile fatty acids (VFA), such as acetate, propionate, and butyrate. In the third phase, all the VFA are transformed into acetate, H_2, and CO_2. The fourth phase involves the conversion of these components by methanogenic archaea into biogas, i.e., a mixture of CH_4, and CO_2. Finally, this process is extended to biological methanation which includes methane production by the biological activity of methanogenic bacteria converting injected H_2, and CO.The model was based on experimental data from the literature (Sun *et al.*, 2021). The entire experiment was carried out in a bioreactor with a working volume (V_{liq}) of $3.75\times10^{-2}\ m^3$ and hydraulic retention time (HRT) of 20 days operating at 37°C for 207 days. The organic loading rate (OLR) was 0.53 $kg_{COD}/m^3 \cdot d$ of glucose with an inlet liquid flowrate $(q_{liq,in})$ of $1.9\times10^{-3}\ m^3/d$ (Chemical Oxygen Demand COD: amount of oxygen needed to degrade the organic matter into CO_2 and H_2O). The gas injection was carried out in five stages, in which the injected gas flowrate $(q_{gas,in})$ and the gas loading rate (GLR) were varied in time. These values and the injected concentration of component i in gas phase $(S^g_{i,in})$ are reported in Table 1.

Table 1: Experimental conditions from literature data without DMO (Sun et al., 2021).

Stage	Time (Day)	Injected gas flowrate $(\boldsymbol{m^3/d})$	Gas loading rate$\times10^{-2}$ $(\boldsymbol{m^3/d})$	Initial concentration gas phase $\times10^{-3}$ $(\boldsymbol{kg_{COD}/m^3})$	
				H_2	CO
First 32 days	1-32	-	-	-	-
I	33-64	0.09	0.75	20.83	38.69
II	65-101	1.44	0.75	1.30	2.42
III	102-135	2.88	1.50	1.30	2.41
IV	136-171	2.88	3.75	3.26	6.04
V	172-207	5.76	3.75	1.63	3.02

An extension of the Anaerobic Digestion Model No. 1 (ADM1_ME) to consider the injection of H_2 and CO to improver CH_4 production was proposed in a previous work (Acosta-Pavas *et al.*, 2022). Here, it is rewriten as,

$$\frac{dS_{gas,i}}{dt} = \frac{q_{gas,in}}{V_{gas}} S^g_{i,in} + N_i \left(\frac{V_{liq}}{V_{gas}}\right) - \frac{q_{gas}}{V_{gas}} S_{gas,i} \quad (1)$$

$$\frac{dS_{liq,j}}{dt} = \frac{q_{liq,in}}{V_{liq}} \left(S^l_{j,in} - S_{liq,j}\right) + \sum_k \beta_{j,k} \mu_k X_k - N_i \quad (2)$$

$$\frac{dX_k}{dt} = \frac{q_{liq,in}}{V_{liq}} \left(X_{k,in} - X_k\right) + Y_{k,j} \mu_k X_k - K_{k,dec} X_k \quad (3)$$

where sub-index i indicates the components H_2, CH_4, and CO in the gas phase; sub-index j indicates the components glucose, butyrate, propionate, acetate, H_2, CH_4, and CO in the liquid phase; and sub-index k indicates the biomass that degraded glucose, butyrate, propionate, acetate, H_2, and CO in liquid phase. V_{gas} is the molar fraction volume, $S^l_{j,in}$ the inlet concentration of component *j* in liquid phase, q_{gas} the outlet gas flowrate, $\beta_{j,k}$ the stoichiometric coefficients, $X_{k,in}$ the inlet concentration of biomass k, μ_k and $K_{k,dec}$ the growth rate and decay constant of biomass *k*, $Y_{k,j}$ the yield of biomass *k,* and N_i the mass transfer rate of component i.

3. Dynamic Multi-objective Optimization Construction as Control Strategy

3.1 Multi-objective Optimization

There are several variables that can be optimized in biological processes, yields, productivities, process times, etc. Most of these variables are often conflicting. Thus, it is necessary to find a trade-off between them. This is called a MO problem. In this case, multiple optimal solutions that satisfy the desired conditions of both variables can be found. This is known as the Pareto optimal set. In general, a MO can be formulated as follows,

$$\min_{x,u,p,t}\{J_1(x,u,p),\dots,J_m(x,u,p)\} \qquad s.t.\begin{cases} dx/dt = f(x,u,p,t) & t\in[0,t_f] \\ f_i(x,u,p,t)\le 0 & i=1,2,\dots,n \\ g_i(x,u,p,t)=0 & i=1,2,\dots,k \\ u^L \le u \le u^U \end{cases} \tag{4}$$

where $J_1,\dots,J_m$ are the m objective functions, x the state variables, f_i and g_i indicate inequality and equality constraints on the variable states, u and p denote the control variables and parameters, and u^L, u^U correspond to the lower and upper bounds of the control variables (Tsiantis *et al.*, 2018).

3.2 Dynamic Optimization as a Model Predictive Control

MPC is one of the most widely used control methods in the industry (Morales-Rodelo *et al.*, 2020). A MPC is an advanced control strategy that solves an optimal control problem at every sampling time. The control uses an explicit model to predict the outputs of the system at a future time by calculating the future control sequences to minimize a cost function (Giraldo *et al.*, 2022). The dynamic optimization (control problem) determines the future control value that minimize a specified performance index, i.e., the input variables, that minimizes the following objective function,

$$\min_{u}\left(\sum_{j=t}^{t+H_p}|y^* - y(t+j|t)|^2 + \sum_{j=t}^{t+H_c} W_u\,\Delta u(t+j|t)^2\right) \qquad s.t.\begin{cases} dx/dt = f(x,u,p,t) \\ f_i(x,u,p,t)\le 0 & i=1,2,\dots,n \\ g_i(x,u,p,t)=0 & i=1,2,\dots,k \\ u^L \le u \le u^U \end{cases} \tag{5}$$

where u is the vector of the control variables, H_p and H_c the prediction and control horizons, $y(t+j|t)$ the output prediction calculated at time instant $t+j$ using the information available at time instant t, y^* a reference trajectory which enables to reach the set point. These variables are determined by the MO, $\Delta u(t+j|t)$ is the control move at time instant $t+j$ calculated using information available at time instant t.

A DMO strategy is proposed to determine the optimal values of the objective functions. This strategy entails five steps. **Step 1 - Model definition**: proposition of the dynamic model representative of the biological process. **Step 2 - Definition of the multi-objective control problem:** definition of the objective functions $J_1,\dots,J_m$ to be maximized/minimized by the MO optimization, the vector of the control variables u, the constraints f_i and g_i, and the bounds u^L and u^U of the control variables in the MO optimization. **Step 3 - Selection of the POP:** determination of the Pareto optimal set $J_1^*,\dots,J_m^*$ and select the POP to be used as the reference trajectory in the dynamic optimization. **Step 4 - Definition of the MPC problem defining a single weighted objective based on the POP:** formulation of an objective function considering the previously identified POP in terms of a MPC problem. Indication of the initial guess values u_0, the constraints f_i and g_i, and the bounds u^L and u^U of the control variables in the dynamic optimization. **Step 5 - Determination of control and optimized variables:** execution of the dynamic optimization and determination of the optimal values of the control and optimized variables at each time.

4. Case Study: Dynamic Multi-objective Optimization in Biomethanation Process

The main objective was to optimize yield (Y) and productivity (P) and to achieve larger values with respect to the ones obtained in the literature (data without DMO). Two control variables were proposed $q_{gas,in}$ and $q_{liq,in}$. The yield Y was defined as the CH_4 outlet flowrate $(q_{gas,CH4})$ produced over the total *COD* kilograms added per day, while productivity P was the ratio between $q_{gas,CH4}$ and V_{liq}, expressed as,

$$Y = \frac{q_{gas,CH4}}{S^l_{su,in}\,q_{liq,in} + S^g_{H2,in}\,q_{gas,in} + S^g_{CO,in}\,q_{gas,in}} \tag{6}$$

$$P = \frac{q_{gas,CH4}}{V_{liq}} \tag{7}$$

4.1 Multi-objective Optimization

In this study, the simulations were run using an Intel® Core i7 8665U 2.11 GHz, 16 GB RAM computer. To obtain the Pareto optimal set for each stage, the *paretosearch* function from MATLAB® was used. The MO was proposed as,

$$\max_{\{q_{gas,in}\,q_{liq,in}\}}(Y,P) \qquad s.t.\begin{cases} Equations\ 2-4 \\ Y \le 0.39\ m^3_{CH4}/kgCOD_{added} \\ 1\times10^{-3} \le q_{gas,in} \le 10\ m^3/d \\ 1\times10^{-3} \le q_{liq,in} \le 0.1\ m^3/d \end{cases} \tag{8}$$

The constrains are reported in equation (8) where equation 1-3 correspond to the model dynamics (ADM1_ME), and 0.39 $m^3_{CH4}/kgCOD_{added}$ represents the theoretical cumulative CH_4 volume at 37°C or 0.35 $m^3_{CH4}/kgCOD_{added}$ at standard temperature and pressure conditions (Filer *et al.*, 2019). The MO was performed for stages I-V. 60 Pareto points were computed for each stage. In which 20, 22, 20, 28, and 23 iterations were executed in 14.65, 19.01, 23.15, 38.29, 56.33 min, respectively. Figure 1A displays the Pareto optimal sets for each stage. In stage I and IV, the Pareto optimal set is far from the experimental value, indicating that optimization can perform a representative change in both optimum variables. For the other stages, the experimental point is in the proximity of the Pareto optimal set, indicating that the experiment was performed to maximize yield. The POP selection was performed by normalizing the Pareto optimal set [0,1] and determining the maximum Euclidean length (d_{max}) from the origin on the normalized coordinates. Other POP were selected to maximize the yield and productivity. The first POP considered maximization of productivity, the second one the maximization of the Euclidean length, and the third one maximization of yield (orange, yellow, and purple squares in Figure 1A). Table 2 summarizes the selected POP for yield and productivity maximization in each stage.

Table 2: Multi-objective optimization results.

Stage	POP for maximum productivity		POP for maximum Euclidean length		POP for maximum yield	
	Yield $(\mathbf{m^3_{CH4}/kgCOD}_{added})$	Productivity $(m^3_{CH4}/m^3_{reactor} \cdot d)$	Yield $(\mathbf{m^3_{CH4}/kgCOD}_{added})$	Productivity $(\mathbf{m^3_{CH4}/m^3_{reactor} \cdot d})$	Yield $(\mathbf{m^3_{CH4}/kgCOD}_{added})$	Productivity $(\mathbf{m^3_{CH4}/m^3_{reactor} \cdot d})$
I	0.3155	0.8011	0.3341	0.7080	0.3443	0.2984
II	0.3156	0.8012	0.3340	0.7107	0.3443	0.2984
III	0.3159	0.8471	0.3330	0.7599	0.3417	0.4042
IV	0.3149	0.9847	0.3308	0.9042	0.3371	0.5940
V	0.3167	0.9844	0.3313	0.8943	0.3371	0.5940

4.2 Dynamic Multi-objective Optimization

To perform the dynamic optimization, the *patternsearch* function from MATLAB® was used. The dynamic optimization problem was proposed as,

$$\min_{\{q_{gas,in}\, q_{liq,in}\}} \left(\sum_{j=t}^{t+H_p} \left(\frac{|Y^* - Y(t)|}{Y^*} \right)^2 + \left(\frac{|P^* - P(t)|}{P^*} \right)^2 + \sum_{j=t}^{t+H_c} W_{u,1}\, \Delta q(t)^2_{gas,in} + W_{u,2}\, \Delta q(t)^2_{liq,in} \right) \quad s.t. \begin{cases} Equations\ 2-4 \\ Y \le 0.39\ m^3_{CH4}/kgCOD_{added} \\ 1\times10^{-3} \le q_{gas,in} \le 10\ m^3/d \\ 1\times10^{-3} \le q_{liq,in} \le 0.1\ m^3/d \end{cases} \tag{9}$$

where $Y(t)$ and $P(t)$ were calculated by using (6) and (7). Y^*, and P^* are the POP values for yield and productivity computed by the MO, $\Delta q(t)^2_{gas,in}$ and $\Delta q(t)^2_{liq,in}$ represent the differences between the injected gas and inlet liquid flowrates before and after each step in the dynamic optimization. $W_{u,1}$ and $W_{u,2}$ are the parameters that weight the importance of the control effort for each input of the optimization.

Five cases were studied to assess the dynamic optimization. **Case 1:** ADM1_ME without DMO (experimental value). **Case 2:** ADM1_ME with DMO (POP for maximum productivity). **Case 3:** ADM1_ME with DMO (POP for maximum Euclidean length). **Case 4:** ADM1_ME with DMO (POP for maximum yield). **Case 5:** ADM1_ME with DMO switching between the maximum productivity (stages I, V), maximum Euclidean length (stages II, III) and maximum yield (stage IV). In all cases, the initial guess (u_0) was $1 \times 10^{-3}\ m^3/d$ for both control variables. The lower and upper bounds of the objective variables Y and P, and the constrains were the same presented in the MO. H_p and H_c were considered equal with values corresponding to the time of each stage (see Table 1).

For cases 2, 3, 4 and 5 the simulation times were 2.12, 3.35, 3.37, and 2.89 min, respectively, in which the weights $W_{u,1}$ and $W_{u,2}$ were manually adjusted to values of 1×10^{-6}. Figure 4 shows the dynamical behavior of optimum and control variables. Regarding case 2 in stage V, the productivity was maximized from 0.419 without DMO to 0.982 $m^3_{CH4}/m^3_{reactor} \cdot d$ with a slightly decrease of yield from 0.334 without DMO to 0.316 $m^3_{CH4}/kgCOD_{added}$ with DMO. The inlet liquid flowrate increased from $1.9\times10^{-3}\ m^3/d$ without DMO to $8.4\times10^{-3}\ m^3/d$ with DMO and remained constant for all stages. The injected gas flowrate increased from 5.76 m^3/d without DMO to 10 m^3/d with DMO in stage V.

In case 3, the yield increased from 0.318 to 0.333 $m^3_{CH4}/m^3_{reactor} \cdot d$ in stage I, but decreased with respect to case 1 in stage V. The productivity increased from 0.419 without DMO to 0.982 in stage V. The inlet liquid flowrate increased from 1.9×10^{-3} m^3/d without DMO to 7.0×10^{-3} m^3/d with DMO in stage V. The injected gas flowrate increased from 5.76 m^3/d without DMO to 8.40 m^3/d with DMO in stage V. In case 4, the yield achieved a value of 0.343 $m^3_{CH4}/m^3_{reactor} \cdot d$ in stage I, but decreased slightly to 0.337 $m^3_{CH4}/m^3_{reactor} \cdot d$ in stage V. The productivity reached a value of 0.59 $m^3_{CH4}/m^3_{reactor} \cdot d$ in stage V. The inlet liquid flowrate increased up to

3.69×10^{-3} m^3/d in stage V. The injected gas flowrate increased from 5.76 m^3/d in case 1 stage V to 8.01 m^3/d in stage V.

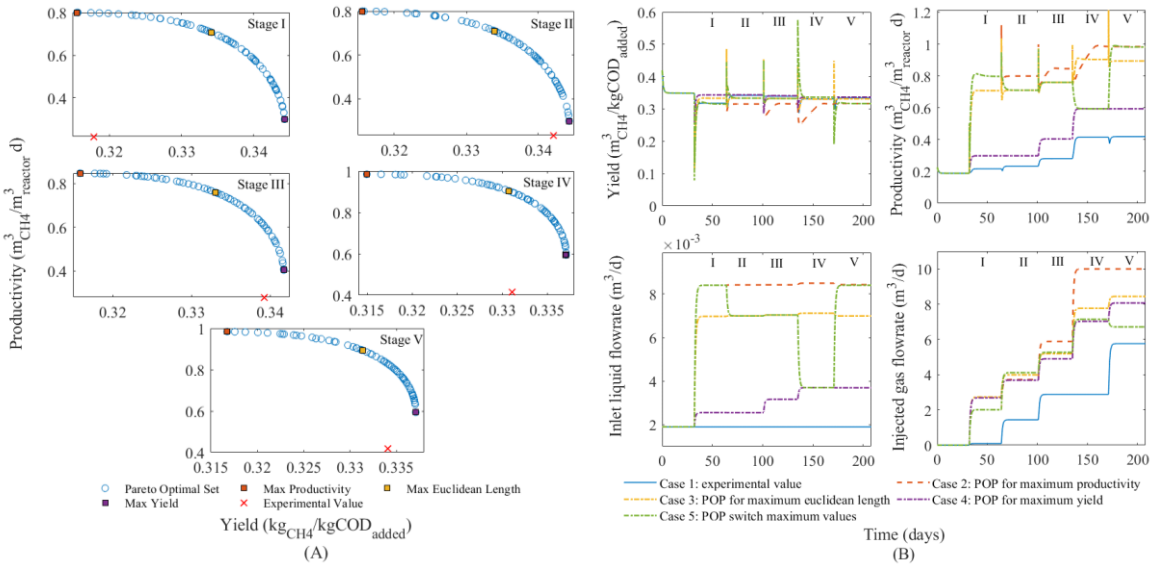

Figure 1: (A) Pareto optimal sets. (B) Yield, productivity, injected gas and inlet liquid flowrates in the DMO.

Table 3: Yield and productivity ratio with DMO.

Stage	Case 1	Case 2		Case 3		Case 4		Case 5	
	Yield $(m^3_{CH4}/kgCOD_{added})$								
	Value	Value	Ratio	Value	Ratio	Value	Ratio	Value	Ratio
I	0.318	0.315	0.99	0.333	1.05	0.343	1.08	0.315	0.99
II	0.342	0.315	0.92	0.333	0.97	0.344	1.00	0.333	0.97
III	0.339	0.316	0.93	0.332	0.98	0.341	1.01	0.332	0.98
IV	0.331	0.315	0.95	0.330	1.00	0.336	1.02	0.336	1.02
V	0.334	0.316	0.95	0.331	0.99	0.337	1.01	0.316	0.95
	Productivity $(m^3_{CH4}/m^3_{reactor} \cdot d)$								
I	0.217	0.807	3.72	0.708	3.26	0.298	1.37	0.798	3.67
II	0.234	0.800	3.42	0.710	3.04	0.298	1.28	0.711	3.04
III	0.28	0.846	3.02	0.76	2.71	0.404	1.44	0.760	2.71
IV	0.415	0.985	2.37	0.904	2.18	0.594	1.43	0.594	1.43
V	0.419	0.982	2.34	0.894	2.13	0.594	1.42	0.982	2.34

In case 5, the yield, productivity, and the inlet liquid flowrate followed the behavior of case 2 in stage I, the behavior of case 3 in stages II and III, the behavior of case 4 in stage IV, and again the behavior of case 2 in stage V. However, the injected gas flowrate differs for all cases and stages.

Table 4 reports the obtained values for yield and productivity as well as a ratio of their respective values with respect to case 1(experimental data). Values larger than 1 show that the DMO is better than the experimental data. For case 2, the yield was 0.99 times higher than the yield for case 1 in stage I and 0.95 times in stage V. On the other hand, the productivity increases 3.72 times and decreases to 2.34 times from stages I to V, respectively.

Concerning case 3, the yield ratio varied between 1.05 and 0.99 times while the productivity ratio changed between 3.26 and 2.13 times concerning without DMO (case 1) for stages I and V, respectively. For case 4, the yield was 1.08 times higher than the yield for case 1 in stage I and 1.01 times in stage V. On the other hand, the productivity increased between 1.28 and 1.44 for the different stages.

For case 2, the inlet liquid flowrate increased slightly, ranging from 1.9×10^{-3} m^3/d (case 1) to a value up to 8.4×10^{-3} m^3/d in stage V. However, the injected gas flowrate needed was higher ranging from the values reported in Table 1 (case 1) to values between 2.69 m^3/d and 10.00 m^3/d between stages I and V. In case 3, to maintain the maximum yield and productivity, the DMO suggested keeping the inlet liquid flowrate at 7.0×10^{-3} m^3/d during all stages while changing the injected gas flowrate between 2.73 and 8.44 m^3/d from stage I to V. For case 4, an inlet liquid flowrate between 2.56×10^{-3} m^3/d and 3.70×10^{-3} m^3/d from stage I to V was used to maintain the maximum yield. The injected gas flowrate ranged between 2.69 and 8.07 m^3/d from stage I to

V. Case 5 followed the same behavior for the inlet liquid flowrate, whereas the injected gas flowrate behavior was different for all cases.

5. Conclusions

In this work, a DMO strategy for the biomethanation process based on the dynamic model ADM1_ME was presented. Optimizations for two objectives were performed: maximization of yield and productivity by modifying the inlet liquid and injected gas flowrates. The proposed strategy showed the conflicting behavior of both objectives. Five cases studies were compared, where it was observed that maximizing productivity lowers yield ratio, and vice versa. Case 5 reported a switching strategy between objectives, which allows to demonstrate the robustness of the process and the well accounted adaptations of the input variables in simulations. Additionally, it was demonstrated that both input variables have a role in DMO. For instance, the injected gas flowrate made a higher effort with respect to the inlet liquid flowrate. This was observed in case 5, where the behavior of the injected gas flowrate differed in all cases. These results show the feasibility of the proposed methodology and its use for multiple control objectives.

Acknowledgments

This research was supported by the Ministerio de Ciencias, Tecnología e Innovación (Minciencias) through the Scholarship Program No. 860.

References

Acosta-Pavas, J. C., Morchain, J., Dumas, C., Ngu, V., Cockx, A., & Aceves-Lara, C. A. (2022). Towards Anaerobic Digestion (ADM No.1) Model's Extensions and Reductions with In-situ Gas Injection for Biomethane Production, Accepted. 10th Vienna International Conference on Mathematical Modelling (MATHMOD), 6.

Batstone, D. J., Keller, J., Angelidaki, I., Kalyuzhnyi, S. V., Pavlostathis, S. G., Rozzi, A., Sanders, W. T. M., Siegrist, H., & Vavilin, V. A. (2002). The IWA Anaerobic Digestion Model No 1 (ADM1). Water Science and Technology, 45(10), 65–73.

Camacho, E. F., & Bordons, C. (2007). Model Predictive control. Springer London. https://doi.org/10.1007/978-0-85729-398-5

Chang, K.-H. (2015). Multiobjective Optimization and Advanced Topics. In e-Design (pp. 1105–1173).

Czatzkowska, M., Harnisz, M., Korzeniewska, E., & Koniuszewska, I. (2020). Inhibitors of the methane fermentation process with particular emphasis on the microbiological aspect: A review. Energy Science and Engineering, 8(5), 1880–1897.

Dar, R. A., Parmar, M., Dar, E. A., Sani, R. K., & Phutela, U. G. (2021). Biomethanation of agricultural residues: Potential, limitations and possible solutions. Renewable and Sustainable Energy Reviews, 135(August 2020), 110217.

Deb, K., Pratap, A., Agarwal, S., & Meyarivan, T. (2002). A fast and elitist multiobjective genetic algorithm: NSGA-II. IEEE Transactions on Evolutionary Computation, 6(2), 182–197.

Filer, J., Ding, H. H., & Chang, S. (2019). Biochemical Methane Potential (BMP) Assay Method for Anaerobic Digestion Research. Water, 11(5), 921.

Giraldo, S. A. C., Melo, P. A., & Secchi, A. R. (2022). Tuning of Model Predictive Controllers Based on Hybrid Optimization. Processes, 10(2), 351.

Morales-Rodelo, K., Francisco, M., Alvarez, H., Vega, P., & Revollar, S. (2020). Collaborative control applied to bsm1 for wastewater treatment plants. Processes, 8(11), 1–22.

Rosen, C., & Jeppsson, U. (2006). Aspects on ADM1 Implementation within the BSM2 Framework. In Technical report.

Sun, H., Yang, Z., Zhao, Q., Kurbonova, M., Zhang, R., Liu, G., & Wang, W. (2021). Modification and extension of anaerobic digestion model No.1 (ADM1) for syngas biomethanation simulation: From lab-scale to pilot-scale. Chemical Engineering Journal, 403(1), 126177.

Tsiantis, N., Balsa-Canto, E., & Banga, J. R. (2018). Optimality and identification of dynamic models in systems biology: An inverse optimal control framework. Bioinformatics, 34(14), 2433–2440.

Vertovec, N., Ober-Blöbaum, S., & Margellos, K. (2021). Multi-objective minimum time optimal control for low-thrust trajectory design.